

## UNSTEADY SURFACE PRESSURE INDUCED BY TURBULENCE OVER ASYMMETRICALLY BEVELED TRAILING EDGE

Yaoyi Guan

Scott C. Morris

Department of Aerospace and Mechanical Engineering  
University of Notre Dame  
119 Hessert Laboratory, Notre Dame, IN 46556 USA  
yguan@nd.edu

Department of Aerospace and Mechanical Engineering  
University of Notre Dame  
110 Hessert Laboratory, Notre Dame, IN 46556 USA  
s.morris@nd.edu

### ABSTRACT

The characteristics of unsteady surface pressure (USP) induced by turbulent flow over a family of asymmetrically beveled trailing edges were studied experimentally. The geometries had a trailing-edge angle  $\theta = 25^\circ$  with a flat lower surface and a rounded upper surface with radii of curvature between 1 and 6 times the airfoil thickness. The chord-based Reynolds number was  $Re = 2.1 \times 10^6$ . A detailed description of the USP and flow fields around the trailing edge section was obtained by remote microphone probes (RMP) and particle image velocimetry (PIV), respectively. The beveled upper surface was characterized by a region of favorable pressure gradient, followed by a strong adverse pressure gradient. The cases with smaller radius of curvature were found to exhibit larger separated region over the trailing edge. The spectral magnitudes of USP were largest in separation region. This paper is focused on scaling and understanding the USP spectra in regions of separated flow. The PIV measurements were utilized to provide the corresponding length and velocity scales.

### Introduction

The characteristics of the unsteady surface pressure (USP) in the trailing edge region of a family of airfoil with various trailing edge geometries are presented in this paper. The experiments for present study employed arrays of remote microphone probes (RMP) to measure the USP, as well as particle image velocimetry (PIV) to obtain velocity statistics of the flow field. The experimental data were utilized to provide insight into the relationships between the trailing edge geometry, the turbulent flow field and the unsteady surface pressure field. These results are of interest for the understanding of aerodynamic noise generated by turbulent flow over lifting surface (Blake (1986)). For example, cooling fans, turbine blade and propellers can generate considerable aerodynamics noise (Roger and Moreau, 2002). In these applications, unsteady surface pressure fluctuations near the trailing edge of the lifting surface can be the dominating noise source at low Mach numbers (Curle, 1955; Amiet, 1976).

The characteristics of turbulence-induced USP have been studied analytically, experimentally, and numerically for over 60 years. Kraichnan (1956) presented one of the earliest studies considering the scaling of the relevant characteristics, such as the mean-square magnitude and correlation length of the fluctuations using a Turbulent Boundary Layer (TBL) over a flat plate with Zero Pressure Gradient (ZPG). Experimentally, several authors assessed the USP below a turbulent boundary layer with ZPG. Willmarth & Wooldridge (1962) pointed out that the spectral magnitude of the USP scaled with the free-stream velocity and the boundary layer displacement thickness. Corcos (1963, 1964) proposed a model for the cross-correlation of the USP under TBL, which was widely applied. Panton & Linebarger (1974) and Chase (1980) determined the wavenumber spectra of the USP for TBL with ZPG. Goody (2004) extensively reviewed previously published USP data over a

large range of Reynolds numbers and proposed an empirical model for the unsteady surface pressure spectrum under TBL with ZPG incorporating the Reynolds number effect. However, flow conditions are often complex in engineering applications. The understanding of the characteristics of the USP field under complex flow conditions, such as favorable pressure gradient (FPG), adverse pressure gradient (APG) and separated flow, were very limited.

Schloemer (1967) studied the USP for a variety of conditions with ZPG, mild APG and FPG experimentally. The study showed that the amplitude of low-frequency USP increased under flow with APG while the high-frequency amplitudes were not affected significantly. In contrast, under the presence of an FPG boundary layer, the high-frequency components of the spectrum showed a faster decay when compared to the case under ZPG flow, while spectral level was slightly higher than in the ZPG flow at low frequencies. Rozenberg & Robert (2012) proposed an empirical model to predict the wall USP spectra for APG flows, which extended the model of Goody (2004) for ZPG flows as discussed above. The authors employed the wake model of Coles (1956) to determine the APG flow parameters and the pressure gradient parameter defined by Clauser (1975) was utilized to quantify the local APG. The results indicated that the displacement thickness and the maximum shear stress were the preferred scaling parameters for the pressure fluctuations under the TBL with APG.

Simpson *et al.* (1987) reported measurements of the wall pressure spectra, wave speeds, and coherence under a separating turbulent boundary layer. The root-mean-square (RMS) of the USP was found to increase monotonically over the attached-flow region with APG and over the separated-flow region. The authors suggested to scale the USP fluctuations with the local maximum of the turbulent shear stress rather than the wall shear stress, which improved the collapse of the data points. Confirming the limitation of the ZPG model addressed by Kraichnan (1956), Simpson *et al.* (1987) noted that the turbulent statistics changed rapidly in the streamwise direction. Ji & Wang (2012) employed Large-Eddy Simulation (LES) to study the flow and USP fields downstream of backward-facing steps. The wall pressure fluctuations under separated shear layer were observed to collapse well in low frequency range while the high-frequency components showed large spread when scaled on the size of the separation bubble. In many applications, the characteristics of the USP over surfaces with complex geometries are of great interest.

The flow encountered around the trailing edge of airfoils and the resulting surface pressure fluctuations are highly dependent on the geometry. Early work on trailing edge flows over sharp and blunt geometries has been reported by Blake (1975) and Blake (1984). The work was focused on a class of asymmetrically beveled trailing edges defined by a flat lower surface and the trailing edge angle  $\theta$  as shown in Figure 1. The curved upper surface was circular with radius  $R$ , and tangent to the horizontal and slanted surfaces. In these studies, an important length scale for trailing edge

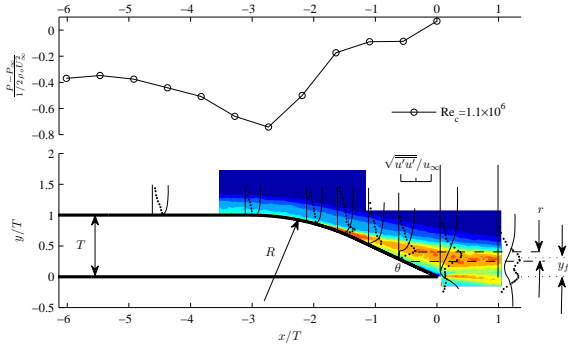


Figure 1. Static pressure distribution over the upper surface of the trailing edge section of the airfoil and contour of streamwise RMS velocity obtained by PIV. —, mean velocity profile; •, RMS velocity profile.

flow, the wake thickness  $y_f$  was proposed and defined as the minimum cross-wake distance between the two local maxima of the root-mean-square of the streamwise velocity, which is shown in Figure 1. Detailed discussion about  $y_f$  can be found in Pröbsting *et al.* (2016). Blake (1984) also stated that the end of vortex formation nearly corresponded to the location of the minimum shear layer spacing and defined  $y_f$  as the minimum distance between the two local maxima of mean streamwise velocity fluctuations in the wake and later adapted this definition for  $y_f$  in the context of beveled trailing edges (Blake, 1986).

Later, the characteristics of the velocity and USP fields were studied experimentally by Shannon & Morris (2006) and Pröbsting *et al.* (2014). Wang & Moin (2000); Wang (2005) and van der Velden *et al.* (2016) studied the flow field around  $25^\circ$  and  $45^\circ$  trailing edge by Large-Eddy Simulation (LES) and Lattice Boltzmann Method (LBM), respectively. Related to the present work, Guan *et al.* (2016b) have described in detail the wake flow of a family of trailing edges with  $\theta = 25^\circ$  and the radius of curvature ranging from  $R/T = 0$  to 10.

Although extensive research has been conducted on turbulence-induced pressure fluctuations, still comparatively little is known about the USP under non-equilibrium flow conditions including APG, FPG, and reverse flow after separation. Figure 1 shows a representation of these complex flow conditions on the upper surface of a beveled trailing edge with  $\theta = 25^\circ$  and  $R/T = 4$ . All these conditions of non-equilibrium flow result in an increased level of the USP. The objective of the present research was to experimentally investigate the characteristics of the unsteady surface pressure field for the family of trailing edge flows exhibiting these conditions to varying extent. To this end, the unsteady surface pressure was measured by arrays of Remote Microphone Probes (RMP) over a family of asymmetrically beveled trailing edges with  $\theta = 25^\circ$ . The models are identical to those described by Guan *et al.* (2016b). These specific trailing edge geometries were selected to create complex flow conditions including FPG, APG and flow separation. The detailed flow statistics provided by Particle Image Velocimetry (PIV) were discussed in Guan *et al.* (2016b), and will be shown briefly here as they provide context and scaling quantities that will be used to better understand the USP measurements.

## Experimental setup

The measurement of the USP presented in this study were conducted in the Anechoic Wind Tunnel (AWT) facility at the University of Notre Dame. The AWT consists of an open-jet test section surrounded by a large anechoic chamber as shown in Figure 2. The

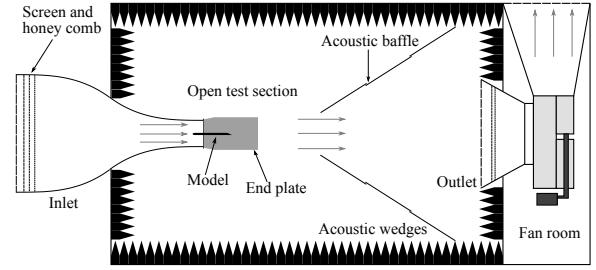


Figure 2. Schematic of the Anechoic Wind Tunnel facility with installation of the model.

walls were covered with glass fiber wedges rated with an absorption coefficient of 99% for  $f > 100\text{Hz}$ . Air was drawn in through a set of turbulence screens, an 8:1 contraction, and a straight section to the nozzle exit with cross section  $0.61\text{m} \times 0.61\text{m}$ . The flow in the test section was constrained on the upper and lower sides by end plates to obtain a 2D mean flow. The airfoil model was mounted vertically at zero incidence in the test section such that the upstream part of the model, up to the quarter-chord point, was placed inside the straight section. At the opposite side of the open chamber, the flow was guided through an acoustically treated section to the primary fan. Specifics regarding the design and construction of the AWT facility can be found in Mueller *et al.* (1992) and Scharpf (1993).

The airfoil models were constructed as a flat strut with a uniform cross section across the span. The cross section of the leading edge component of the airfoil was a five-to-one aspect ratio semi-ellipse. The middle section of the model was a flat plate with 5.04 cm thickness. The trailing-edge component was exchangeable. The trailing edge angle was  $\theta = 25^\circ$ . The values of the ratio of the radius of curvature of the upper-surface beveled part to airfoil thickness were  $R/T = 1, 2, 4$  and 6, respectively. The geometries of the different trailing edge sections are shown in Figure 3. More details of the airfoil model geometry and the PIV setup were provided by Guan *et al.* (2016b).

For all experiments, the free-stream velocity was set to roughly  $35\text{m/s}$ , corresponding to a chord-based Reynolds number of  $Re_C = 2.1 \times 10^6$ . The boundary layer was tripped on either side of the airfoil at the location quarter chord downstream of the leading edge. The boundary layer thickness and displacement thickness at  $x/T = -5.5$  were found to be  $\delta_{99} = 8.6\text{mm}$  and  $\delta^* = 1.2\text{mm}$ , respectively, as measured by single-sensor hot-wire anemometer.

Measurement of the USP were acquired by the use of remote microphone probes (RMP). The details about the structure, manufacture and calibration of the RMP were described by Guan *et al.* (2016a). This measurement technology was previously utilized to measure the wall pressure fluctuations by Pröbsting *et al.* (2014), Bilka *et al.* (2015) and van der Velden *et al.* (2016). The streamwise microphone array on the upper surface of the trailing edge section was located in the middle span. The streamwise coordinates of each element of the RMP array on different trailing edge geometries were shown in Table 1. Data were acquired at a scanning frequency of  $40\text{kHz}$  for a period of 52.4s

## Results and discussion

### 0.1 Characteristics of flow field

Prior to the detailed discussion of the unsteady pressure, it is useful to consider the general characteristics of the mean flow and pressure field in the vicinity of the airfoil trailing edge. Figure 1 shows the geometry, the static pressure distribution, and contours of the streamwise root-mean-square velocity on the upper surface for the  $R/T = 4$  geometry. The upper-surface flow encountered a favorable pressure gradient, followed by adverse pressure gradient.

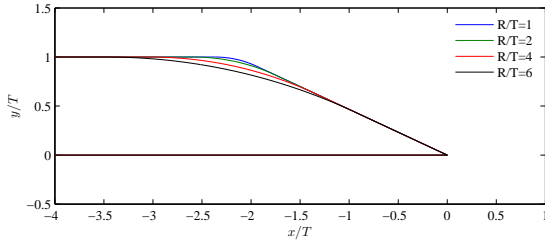


Figure 3. The family of  $\theta = 25^\circ$  asymmetrically beveled trailing edge for  $R/T = 1, 2, 4$  and  $6$ .

Table 1. Streamwise coordinates  $x_m/T$  of the individual elements of the RMP array on the upper surface of the trailing edges.

$R/T =$	1	2	4	6
A	-1.39	-1.50	-1.51	-1.52
B	-0.82	-0.87	-0.88	-0.88
C	-0.53	-0.56	-0.57	-0.57
D	-0.39	-0.41	-0.41	-0.42
E	-0.32	-0.34	-0.34	-0.34
F	-0.28	-0.30	-0.30	-0.30
G	-0.26	-0.29	-0.29	-0.29

The turbulent boundary layer thickness was observed to increase significantly in the APG region. Flow separation was observed near  $x/T = -1.1$  and  $y/T = 0.5$ . A free shear layer developed from the separation point. A recirculation region was bounded by the free shear layer and the rigid surface. A second shear layer originating from the lower surface corner separation can be observed. Additional details of the flow physics for this and other  $R/T$  values was provided by Guan *et al.* (2016b). Of interest includes the large-scale coherent motions observed in the wake. The size of these motions was found to be proportional to the wake thickness  $y_f$ , which decreased with increasing  $R/T$ . This was because the separation point was found to move downstream as the value of  $R/T$  increased.

## 0.2 Effect of the geometry on surface pressure spectra

The upper surface spectra from the  $R/T = 1, 4$  and  $6$  case are shown in Figure 4 a), b) and c), respectively. The streamwise coordinates  $x_m/T$  of each element of the RMP array are shown in Table 1. The pressure spectra are normalized by airfoil thickness  $T$  and free-stream velocity  $u_\infty$ . For comparison, the pressure spectra of the USP under TBL with ZPG measured at upstream locations are included (red dashed line).

The spectral amplitudes in the low frequency range increased for locations closer to the trailing edge for all geometries. For example, the value of spectral magnitude at  $fT/u_\infty = 0.3$  at station G is 13dB higher than that at station A for  $R/T = 4$  case. In contrast, the high-frequency components are found to decrease in downstream direction. The value of spectral magnitude at  $fT/u_\infty = 5$  at station G is 28dB lower than that at station A for  $R/T = 4$  case. Complex changes in the spectral amplitudes can be observed, depending on whether the flow was fully attached, separating or separated. These

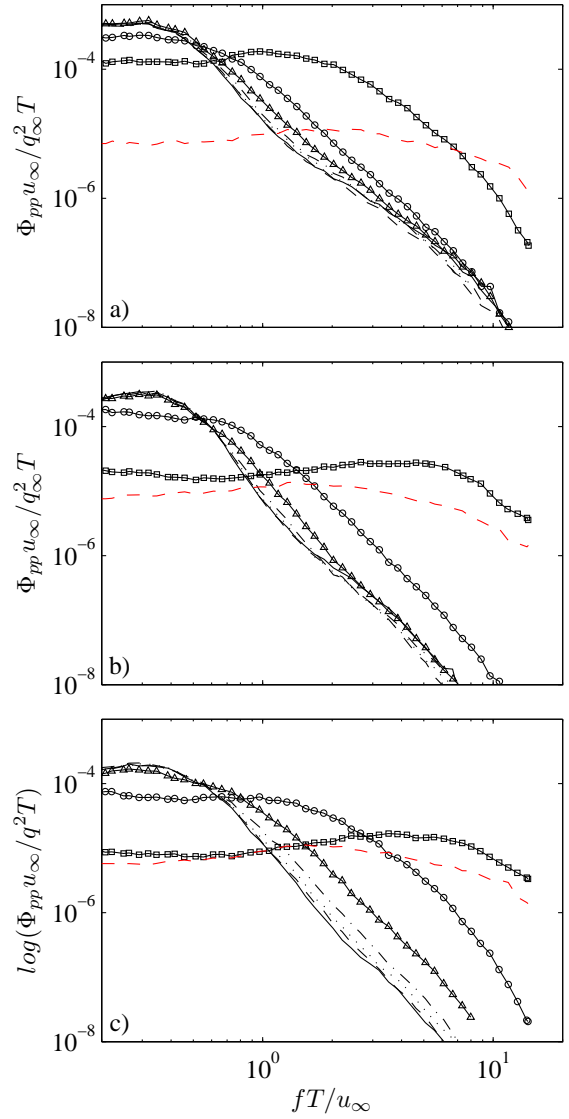


Figure 4. USP auto-spectral density on the upper surface near the trailing edges at various streamwise locations for  $Re_C = 2.1 \times 10^6$ , a)  $R/T=1$ , b)  $R/T=4$ , c)  $R/T=6$ .  $\square$ -, A;  $\circ$ -, B;  $-\Delta$ -, C;  $-\cdot-$ , D;  $\cdots$ -, E;  $-\cdot-$ , F;  $-\cdot-$ , G;  $-\cdot-$ , USP under turbulent boundary layer with ZPG

details are discussed in the following.

For all trailing edge geometries, the spectra show a general trend where the local maximum increases in magnitude and decreases in frequency as the observation point approaches the trailing edge. For  $R/T = 4$  case, the local maximum was observed at  $fT/u_\infty = 0.3$  with spectral magnitude of  $3.5 \times 10^{-4}$  at station G while for station A the local maximum appeared at  $fT/u_\infty = 2.7$  with spectral magnitude of  $2.8 \times 10^{-5}$ . Similar results were observed in the cases of  $R/T = 1$  and  $6$ , which are shown in Figure 4 a) and c), respectively. This generally led to increases in low-frequency amplitude that were between 10 and 15 dB higher than the approaching boundary layer, with concomitant decreases in high-frequency amplitude as large as 15 to 30 dB depending on the geometry. These observations are consistent with expectations based on the flow fields shown in Figure 1. Specifically, as the boundary layer thickens due to the APG and finally separates, the large-scale motions that develop in the shear layer create the increases in the lower frequency range. The observed decreases

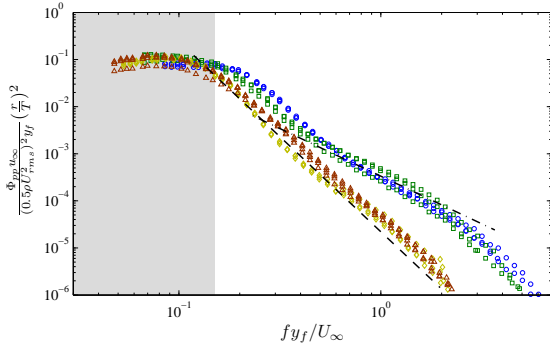


Figure 5. The spectral density of USP under separated flow, normalized by wake length scale

at high frequency are a result of the distance between the shear-induced small-scale motions and the surface after separation.

### 0.3 Scaling of surface pressure below separated flow

The preceding discussion illustrated the large difference in magnitude of the surface pressure fluctuations that occurred for the varied streamwise locations and  $R/T$  values considered. It is now of interest to consider how the pressure fluctuations scale with local or global flow characteristics in order to better quantify the physical cause of the observations. The scaling of the UPS under attached flow with FPG, ZPG and APG has been studied intensively by Schloemer (1967), Goody (2004) and Rozenberg & Robert (2012). In the present study, the region with separated flow will be described. The characteristics of USP fluctuations are distinctly complex in the separated region, and hence a single set of scaling parameters was not found to be sufficient to collapse the spectra. Analysis of the data has led to three distinct regions in the frequency domain, each with a different type of scaling.

First, the spectra from each  $R/T$  case with locations within the separated zone only are shown in Figure 5. The spectra were normalized using the time scale  $y_f/u_\infty$ , the pressure scale associated with the local maximum streamwise turbulence intensity in the separated shear layer  $0.5\rho u^2$ . This result was then further scaled by the vertical distance between the surface microphone and the center of the detached shear layer,  $r$ , which is indicated in Figure 1. This location was determined by the maximum streamwise root mean square velocity observed in the PIV data. A schematic representation of this is shown in Figure 1 for  $R/T = 4$  at a single microphone location. The results shown indicate a reasonable collapse of all the USP spectra under separated flow at dimensionless frequencies  $f y_f / u_\infty < 0.10$ . In this range the amplitudes were found to be nearly constant, or "flat" with respect to frequency. Near  $f y_f / u_\infty = 0.15$ , all of the spectra exhibited a change to a distinctly negative slope, which was shown by the black dashed line. The roll-off slopes started to vary for different geometries and streamwise locations at  $f y_f / u_\infty = 0.3$ . The values of slopes of the spectra can be observed to be different for the various geometries and spatial locations as shown by the black dashed line and the dotted-dashed line.

The agreement of the spectra through  $f y_f / u_\infty < 0.15$  with the indicated scaling provides some insights into the nature of the turbulence that led to the pressure fluctuations. First, the use of the maximum streamwise turbulence intensity of the shear layer, as well as the local distance to the center of the shear layer, indicates that the USP was caused by the turbulence directly "above" the observation point. The use of the wake time scale,  $y_f / u_\infty$ , is interesting and

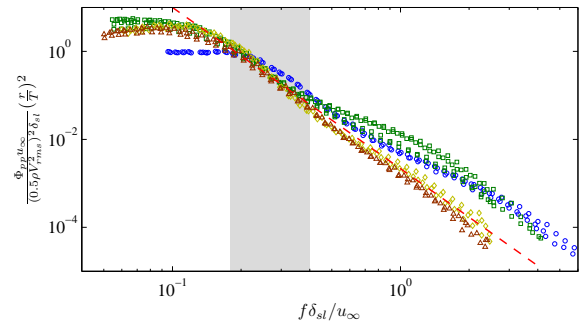


Figure 6. The spectral density of USP under separated flow, normalized by wake length scale

can be understood by considering the convective length scale in this frequency range. Specifically, the value of  $f y_f / u_\infty = 0.1$  can be interpreted to indicate that the streamwise length scale of these motions was 10 times larger than the size of the wake. Hence, the time scale of the fluctuations at these very low frequency values could not be associated with the local shear layer that was generally a fraction of  $y_f$  in scale. In summary, the mixed scaling indicates that the local USP fluctuations are primarily caused by the small-scale turbulence in the shear layer, but the shear layer is modulated by the large-scale fluctuations in the wake, which was discussed by Guan *et al.* (2016b). This modulating influence of the the large-scale fluctuations on the shear layer turbulence has also been described by Shannon & Morris (2006). Similar phenomena were reported by Ji & Wang (2012) who studied the surface pressure fluctuations downstream of backward-facing steps.

The scaling of the middle frequency range is shown in Figure 6. The auto-spectral density of the USP was normalized with the time scale  $\delta_{sl}/u_\infty$  associated with the convecting fluctuations in the local, separated shear layer. The length scale of the shear layer,  $\delta_{sl}$ , at a certain streamwise location is defined as the vertical distance between the two points at which the values of the vertical RMS velocity,  $\overline{v^2}^{-1/2}$ , are half as large as the maximum value of  $\overline{v^2}^{-1/2}$  at the same streamwise location. The amplitude was normalized using the maximum  $\overline{v^2}^{-1/2}$  values identified directly above the microphone location using the PIV data. As before, the amplitudes were further normalized using the vertical distance between the wall and the center of the separated shear layer  $r$ . This location was determined by the maximum vertical root mean square velocity observed in the PIV data. With this selection of scales, the spectra show a collapse over a mid-frequency range between  $0.2 < f \delta_{sl} / u_\infty < 0.4$  (Figure 6, shaded region). The slope of the pressure spectra in middle frequency range was found to be approximately  $-11/3$  as shown by the red dashed line. Some of the spectra, primarily from the  $R/T = 4$  and 6 cases, roughly followed this slope out to the highest frequencies that were measured. Other cases, notably the  $R/T = 1$  and 2 cases, indicated significant departures from the  $-11/3$  slope, with larger amplitudes in the high frequency range.

Careful inspection of the spectra and PIV data led to the hypothesis that the geometries with the most significant flow separation (i.e.,  $R/T = 1$  and 2) resulted in significant reverse-flow at the surface, and that the turbulence associated with this reverse flow led to the varied spectral amplitudes at high frequency range. This idea was tested by considering the phase of the cross-spectral density,  $\phi$ , between closely spaced microphones near the trailing edge. The phase values between microphone locations F and G on the upper surface are shown in Figure 7. Positive phase shift should indicate that the fluctuation-producing structures are convecting down-

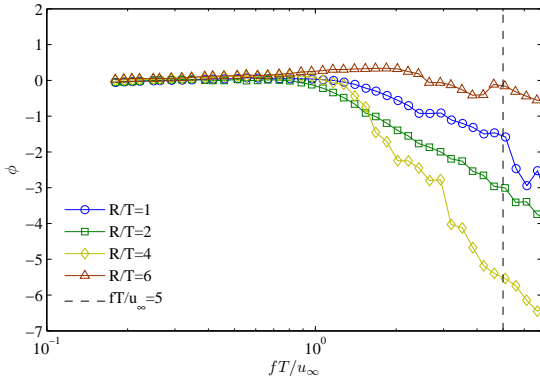


Figure 7. phase shift of USP cross-spectral density

stream. For the cases with fully separated shear layer and reverse flow at this location ( $R/T = 1$  through 6)  $\phi$  is close to 0 at low frequency range and decreases to negative values at high frequencies. This negative phase shift indicates flow moving in the upstream direction at high frequencies as suggested.

The results presented demonstrate that the lower  $R/T$  cases exhibit high-frequency USP amplitudes that are related to reverse flow at the surface. It is also of interest to compare the amplitude of the spectra with the speed of the reverse flow boundary layer. This was not possible using the PIV data, as the reverse flow boundary layer was found to be very near to the surface, and hence in a region where the PIV uncertainty was relatively large. As an alternative, a convection velocity was defined from the  $\phi$  values as

$$u_c(f) = \frac{\Delta x \omega}{\phi} \quad (1)$$

The spectral magnitude of the USP at  $fT/u_\infty = 5$  decreased as  $R/T$  increased from 1 to 6 as shown in Figure 8 a) while the magnitude of the negative convection speed at that frequency decreased as shown in Figure 8 b). Note that  $R/T = 6$  was found to have a phase shift very close to zero at this frequency, indicating nearly stagnant mean flow and an undefined  $u_c$  value. This geometry also corresponded to the minimum USP amplitude at higher frequencies. These results indicate that the reverse flow with larger speed led to higher levels of surface pressure fluctuations. Scaling of the USP spectral density at high frequency range was not investigated in present study because of the lack of valid velocity data very close to the wall in the recirculation region.

## Conclusions and future work

The characteristics of the USP under complex flow conditions for a family of asymmetrically beveled geometries with trailing-edge angle  $\theta = 25^\circ$  has been studied in detail. The local characteristics of USP were found to be highly dependent on the flow features present for a particular geometry.

The characteristics of the upper-surface unsteady pressure field were complex because of the strong non-equilibrium flow conditions. The characteristics of the pressure fluctuations under separated flow showed great variety and were dominated by various flow regimes in different frequency ranges. The low-frequency spectral density of USP under separated shear layer collapsed when normalized by a time scale  $y_f/u_\infty$  and a pressure scale  $\rho/2u'^2_{max}$ . This mixed scaling indicated that the magnitude of the low-frequency pressure fluctuations were dominated by the turbulence intensity in the local shear layer, but the frequency of the large-scale oscillations was governed by the turbulent wake. The mid-frequency range of

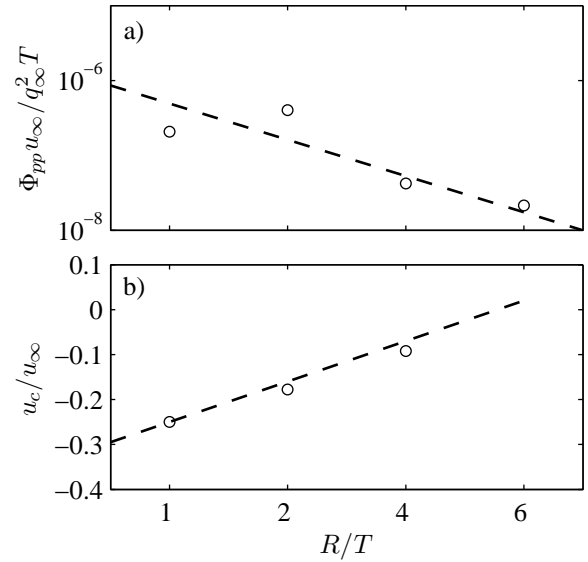


Figure 8. USP spectral magnitude (a) and convection velocity  $u_c$  (b) at  $fT/u_\infty = 5$  for different trailing edge geometries.

the pressure fluctuations collapsed to a significant degree when normalized using the local shear layer thickness  $\delta_{sl}$  and a pressure scale  $\rho/2v'^2_{max}$ . The collapse indicated that the pressure fluctuations in mid-frequency range were dominated by the characteristics of local shear layer. The high-frequency content of the pressure fluctuations under separated shear layer with reverse flow was dominated by upstream-convecting turbulence created by reverse flow. The magnitude of the reverse flow-induced pressure fluctuations increased with faster negative phase speed. The scaling of the USP spectral density at high frequency range, which was dominated by reverse flow, will be studied based on numerical simulation.

Future work involving the trailing edge flow and pressure field will include characteristics of the spanwise correlation length scales of the USP. This is an important topic as it significantly influences the aerodynamic noise generated by the trailing-edge flow. The cross-correlation of the USP on upper and lower surface will also be investigated as it can be an important contributor to the trailing-edge noise.

## Acknowledgements

This research was supported by the U.S. Office of Naval Research (ONR), under grant numbers N00014-09-1-0050 and by the European Community's Seventh Framework Programme (FP7/2007-2013) under the AFDAR project (Advanced Flow Diagnostics for Aeronautical Research), grant agreement No.265695.

## REFERENCES

- Bilka, M. J., Paluta, M. R., Silver, J. C. & Morris, S. C. 2015 Spatial correlation of measured unsteady surface pressure behind a backward facing step. *Experiments in Fluids* **56** (37).
- Blake, W. K. 1975 A statistical description of pressure and velocity fields at the trailing edges of a flat strut. Technical report TR-4241. David W. Taylor Naval Ship Research and Development Center.
- Blake, W. K. 1984 Trailing edge flow and aerodynamic sound, part1. tonal pressure and velocity fluctuations, part 2. random pressure and velocity fluctuations. Technical report DTNSRDC-83/113. David W. Taylor Naval Ship Research and Development Center.

- BLAKE, W. K., ed. 1986 *Mechanics of Flow Induced Sound and Vibration*. Academic Press.
- Chase, D. M. 1980 Modeling the wavevector-frequency spectrum of turbulent boundary layer wall pressure. *Journal of Sound and Vibration* **70** (1), 29–67.
- Clauser, F. H. 1975 Turbulent boundary layers in adverse pressure gradients. *Journal of the Aeronautical Sciences* **21** (2), 91–108.
- Coles, D. 1956 The law of the wake in the turbulent boundary layer. *Journal of Fluid Mechanics* **1** (2), 191–226.
- Corcos, G. M. 1963 Resolution of pressure in turbulence. *The Journal of the Acoustical Society of America* **35** (2), 192–199.
- Corcos, G. M. 1964 Structure of turbulent pressure field in boundary-layer flows. *Journal of Fluid Mechanics* **18** (3), 358–378.
- Goody, M. 2004 Empirical spectral model of surface pressure fluctuations. *AIAA Journal* **42** (9), 1788–1794.
- Guan, Yaoyi, Gerntsen, Carl R., Bilka, Michael J. & Morris, Scott C. 2016a The measurement of unsteady surface pressure using a remote microphone. *Journal of Visualized Experiments* **118**.
- Guan, Y., Pröbsting, S., Stephens, D., Gupta, A. & Morris, S. C. 2016b On the wake flow of asymmetrically beveled trailing edges. *Experiments in Fluids* **57** (78).
- Ji, M. & Wang, M. 2012 Surface pressure fluctuations on steps immersed in turbulent boundary layers. *Journal of Fluid Mechanics* **712**, 471–504.
- Kraichnan, R. H. 1956 Pressure fluctuations in turbulent flow over a flat plate. *The Journal of the Acoustical Society of America* **28**, 378–390.
- Mueller, T. J., Scharpf, D., Batill, S., Strebinger, R., Sullivan, C. & Subramanian, S. 1992 The design of a low-noise, low-turbulence wind tunnel for acoustic measurements. In *Proceedings of the 28th Joint Propulsion Conference and Exhibit*, pp. 1992–3883. Nashville, USA: AIAA.
- Panton, R. L. & Linebarger, J. H. 1974 Wall pressure spectra calculations for equilibrium boundary layers. *Journal of Fluid Mechanics* **65** (2), 261–287.
- Pröbsting, S., Gupta, A., Scarano, F., Guan, Y. & Morris, S. C. 2014 Tomographic PIV for beveled trailing edge aeroacoustics. In *Proceedings of the 20th AIAA/CEAS Aeroacoustics Conference*, pp. 2014–3301. Atlanta, USA: AIAA.
- Pröbsting, S., Zamponi, M., Ronconi, S., Guan, Y. & Morris, S.C. 2016 Vortex shedding noise from a beveled trailing edge. *International Journal of Aeroacoustics* **15** (8).
- Rozenberg, Y. & Robert, G. 2012 Wall-pressure spectral model including the adverse pressure gradient effects. *AIAA Journal* **50** (12), 2168–2179.
- Scharpf, D. F. 1993 An experimental investigation of propeller noise due to turbulence ingestion. Phd thesis, University of Notre Dame.
- Schloemer, H. 1967 Effects of pressure gradients on turbulent-boundary-layer wall-pressure fluctuations. *The Journal of the Acoustical Society of America* **42** (1), 93–113.
- Shannon, D. W. & Morris, S. C. 2006 Experimental investigation of a blunt trailing edge flow field with application to sound generation. *Experiments in Fluids* **41** (5), 777–788.
- Simpson, R. L., Ghodbane, M. & McGrath, B. E. 1987 Surface pressure fluctuations in a separating turbulent boundary layer. *Journal of Fluid Mechanics* **177**, 167–186.
- van der Velden, W.C.P., Pröbsting, S., van Zuijlen, A.H., de Jong, A.T., Guan, Y. & Morris, S.C. 2016 Numerical and experimental investigation of a beveled trailing-edge flow field and noise emission. *Journal of Sound and Vibration* **384**, 113–129.
- Wang, M. 2005 Computation of trailing-edge aeroacoustics with vortex shedding. Annual research briefs. Center for Turbulence Research, Stanford University.
- Wang, M. & Moin, P. 2000 Computation of trailing-edge flow and noise using large-eddy simulation. *AIAA Journal* **38** (12), 2201–2209.
- Willmarth, W. W. & Wooldridge, C. E. 1962 Measurements of fluctuating pressure at wall beneath thick turbulent boundary layer. *Journal of Fluid Mechanics* **14** (2), 187–210.